NASA Technical Memorandum 82639

Surface Roughness Effect on Finite Oil Journal Bearings

B. C. Majumdar and B. J. Hamrock
Lewis Research Center
Cleveland, Ohio

Prepared for the
International Conference on Optimum Resources Utilization through Tribo-Terotechnology and Maintenance Management at the Indian Institute of Technology
New Delhi, India, November 30-December 6, 1981

NASA

SURFACE ROUGHNESS EFFECT ON FINITE OIL JOURNAL BEARINGS

B. C. Majumdar* and B. J. Hamrock

National Aeronautics and Space Administration

Lewis Research Center

Cleveland, Ohio 44135

SUMMARY

A theoretical study of the performance of finite oil journal bearings is made considering the surface roughness effect. The total load-supporting ability under such a condition derives from the hydrodynamic as well as asperity contact pressure. These two components of load are calculated separately. The average Reynolds equation for partially lubricated surfaces is used to evaluate hydrodynamic pressure. An analytical expression for average film thickness is obtained and introduced to modify the average Reynolds equation. The resulting differential equation is then solved numerically by finite difference methods for mean hydrodynamic pressure, which in turn gives the hydrodynamic load. Assuming the surface height distribution as Gaussian, the asperity contact pressure is found. The effect of surface roughness parameter, surface pattern, eccentricity ratio, and length-to-diameter ratio on hydrodynamic load and on side leakage is investigated. It is shown that hydrodynamic load increases with increasing surface roughness when both journal and bearing surfaces have identical roughness structure or when the journal only has a rough surface. The trend of hydrodynamic load is reversed if the journal surface is smooth and the bearing surface is rough.

E-894

---

*National Research Council - NASA Lewis Research Center Associate.

INTRODUCTION

The first step in gaining insight into the lubrication of solid surfaces is to examine the surface profile or topography. Smooth surfaces are not flat on an atomic scale. The roughnesses of manufactured surfaces used in lubrication are between 1×10^{-8} and 20×10^{-8} m, whereas typical atomic diameters are between 1×10^{-10} and 10×10^{-10} m. Even a highly polished surface, when examined microscopically or with a profilometer, has an irregular nature. The surface consists of high and low spots. The high spots, or protuberances, are also called asperities.

When the bearing surfaces are not perfectly smooth, there is a possibility of asperity contact. The contact pressure thus developed on asperities will carry a part of the applied load. As the surfaces will have relative motion under lubrication, hydrodynamic pressure will also be generated as a result of wedge action and the viscosity of the lubricant. A few theories for predicting the surface contact pressure of nominally flat surfaces are available [1-4]. There are two main approaches [5,6] for calculating the hydrodynamic load of partially lubricated surfaces. Patir and Cheng [5] used the flow simulation method of a randomly generated rough surface with known statistical properties over the surface area. Tønder [6] studied the lubrication of a rough surface by a Monte Carlo method. In an earlier report the authors [7] have estimated the mean hydrodynamic and contact loads of rough surface plane sliders and infinitely long journal bearings with both surfaces having identical roughness structures. As both the surfaces had the same roughness structure, the shear flow effect was neglected in [7].

The objective of the present paper is to study the surface roughness effect on finite journal bearings where the two surfaces have different roughness structures. The present work uses a flow model similar to that of

Patir and Cheng [5], but the average gap height is obtained analytically. This is then introduced to modify the governing differential equation. The contact load is computed by using a model given by Greenwood and Tripp [4]. The partial differential equation for mean hydrodynamic pressure is solved numerically by finite difference methods satisfying Reynolds boundary conditions. The hydrodynamic load, attitude angle, and side leakage are found for various length-to-diameter ratios, eccentricity ratios, roughness parameters, surface patterns, and variance ratios. The effect of these design parameters on hydrodynamic load and side leakage is discussed.

NOTATION

C	nominal radial clearance [m]
D	journal diameter [m]
E	modulus of elasticity of bearing material [N/m^2]
E'	composite modulus of elasticity of two surfaces [N/m^2], $\frac{1}{E'} = \frac{1}{2}\left(\frac{1-\nu_j^2}{E_j} + \frac{1-\nu_b^2}{E_b}\right)$
e	eccentricity [m]
h,H	nominal film thickness [m], $H = h/C$
h_T	average film thickness [m]
K	a constant
L	bearing length [m]
n	number of asperities per unit area
p,P	mean hydrodynamic pressure [N/m^2], $P = pC^2/6\eta uR$
p_c	contact pressure [N/m^2]
q,Q	side leakage [m^3/s], $Q = (L/D)q/CRu$
R	journal radius [m]

u	velocity of surface [m/s], $u = u_j$, $u_b = 0$
V_r	variance ratio, $V_{rj} = (\sigma_j/\sigma)^2$, $V_{rb} = (\sigma_b/\sigma)^2$
w_c, W_c	contact load [N], $W_c = w_c/LDE'$
w_h, W_h	hydrodynamic load [N], $W_h = w_h C^2/6\eta LR^2 u$
x, y, z, Y	coordinates [m], $Y = y/(L/2)$
β	mean radius of curvature of asperities [m]
γ	surface pattern parameter
δ	combined roughness [m], $\delta = \delta_j + \delta_b$
δ_j, δ_b	roughness amplitude of journal and bearing surfaces
ε	eccentricity ratio, $\varepsilon = e/C$
η	absolute viscosity of lubricant [N s/m^2]
θ, θ_2	angular coordinate [rad], $\theta = x/R$, θ_2 = angular coordinate where film breaks
Λ	roughness parameter, $\Lambda = C/\sigma$
ν	Poisson's ratio
σ	standard deviation of combined roughness, $\sigma = \sqrt{\sigma_j^2 + \sigma_b^2}$
σ_j, σ_b	standard deviation of journal and bearing surfaces
ϕ_s	shear flow factor associated with two surfaces
ϕ_x, ϕ_y	pressure flow factors
ϕ_s	shear flow factor associated with single surface
ψ	attitude angle [rad]

Subscripts:

b	bearing surface
j	journal surface

THEORETICAL ANALYSIS

The average Reynolds equation for partial hydrodynamic lubrication has been derived by Patir and Cheng [5], and it can be written after neglecting the local squeeze term for a journal bearing (fig. 1) as

$$\frac{\partial}{\partial x}\left(\phi_x \frac{h^3}{12\eta}\frac{\partial p}{\partial x}\right) + \frac{\partial}{\partial y}\left(\phi_y \frac{h^3}{12\eta}\frac{\partial p}{\partial y}\right) = \frac{u_j + u_b}{2}\frac{\partial h_T}{\partial x} + \frac{u_j - u_b}{2}\sigma\frac{\partial \phi_s}{\partial x} \tag{1}$$

where h_T is given by

$$h_T = \int_{-h}^{\infty} (h + \delta) f(\delta) d\delta \tag{2}$$

and $f(\delta)$ is the probability density function of combined roughness δ.

The flow factors ϕ_x and ϕ_y will approach 1 as h/σ approaches ∞, whereas ϕ_s will be equal to 0 for a large value of h/σ. The flow factors ϕ_x, ϕ_y, and ϕ_s not only depend on h/σ, but are also functions of the statistical properties of the frequency density of roughness heights and the directional properties of asperities. The flow factors ϕ_x, ϕ_y, and ϕ_s were obtained by Patir and Cheng [8] through flow simulation of a rough surface having Gaussian distribution of surface height. These factors are used in the present calculation. The average gap height h_T is calculated in the following way:

For a Gaussian distribution, the normal probability density function of δ is

$$f(\delta) = \frac{1}{\sigma\sqrt{2\pi}} e^{-\delta^2/2\sigma^2} \tag{3}$$

Substituting equation (3) into equation (2) gives

$$h_T = \frac{1}{\sigma\sqrt{2\pi}} \int_{-h}^{\infty} (h + \delta) e^{-\delta^2/2\sigma^2} d\delta \tag{4}$$

After performing integration,

$$h_T = \frac{h}{2}\left[1 + \operatorname{erf}\left(\frac{h}{\sqrt{2}\sigma}\right)\right] + \frac{\sigma}{\sqrt{2\pi}} e^{-h^2/2\sigma^2}$$

Differentiating h_T with respect to x, we get

$$\frac{\partial h_T}{\partial x} = \frac{1}{2}\left[1 + \operatorname{erf}\left(\frac{h}{\sqrt{2}\sigma}\right)\right]\frac{\partial h}{\partial x} \tag{5}$$

The flow factors ϕ_x and ϕ_y are given by

$$\phi_x = 1 - c_1 e^{-r(h/\sigma)} \qquad \text{for } \gamma \leq 1$$

$$\phi_x = 1 + c_1\left(\frac{h}{\sigma}\right)^{-r} \qquad \text{for } \gamma > 1$$

and

$$\phi_y\left(\frac{h}{\sigma}, \gamma\right) = \phi_x\left(\frac{h}{\sigma}, \frac{1}{\gamma}\right)$$

where c_1 and r are constants which can be found in [8] and γ is defined as the ratio of lengths at which autocorrelation functions of the x and y profiles reduce to 50 percent of the initial value. This γ can be thought of as the length-to-width ratio of a representative asperity. Per the definition, purely transverse, isotropic, and longitudinal roughness patterns correspond to γ of 0, 1, and ∞, respectively.

Knowing the flow factors and h_T and assuming $u_b = 0$ and $u_j = u$, we can write equation (1) for a constant n as

$$\frac{\partial}{\partial x}\left(\phi_x h^3 \frac{\partial p}{\partial x}\right) + \frac{\partial}{\partial y}\left(\phi_y h^3 \frac{\partial p}{\partial y}\right) = 6nu\left\{\frac{1}{2}\left[1 + \operatorname{erf}\left(\frac{h}{\sqrt{2}\sigma}\right)\right]\right\}\frac{\partial h}{\partial x} + 6nu\sigma\frac{\partial \phi_s}{\partial x} \tag{5}$$

When h/σ approaches a large value (i.e., for smooth surfaces), equation (6) reduces to the classical two-dimensional Reynolds equation. It has been found that if $h/\sigma \geq 6$, the surface roughness effect can be neglected. Hence a surface having $h/\sigma = 6$ corresponds to a smooth surface.

Patir and Cheng [8] have shown that the shear flow factor ϕ_s can be represented by the following relationship, which is valid when $\gamma_j = \gamma_b$:

$$\phi_s = (V_{rj} - V_{rb})\phi_s$$

where

$$V_{rj} = \left(\frac{\sigma_j}{\sigma}\right)^2$$

and

$$V_{rb} = \left(\frac{\sigma_b}{\sigma}\right)^2$$

$$V_{rb} = 1 - V_{rj}, \text{ since } \sigma = \sqrt{\sigma_j^2 + \sigma_b^2}$$

Substituting $V_{rb} = 1 - V_{rj}$ in the above expression of ϕ_s,

$$\phi_s = (2V_{rj} - 1)\phi_s$$

$$\phi_s = A_1 \left(\frac{h}{\sigma}\right)^{\alpha_1} e^{-\alpha_2(h/\sigma)+\alpha_3(h/\sigma)^2} \qquad \text{for } \frac{h}{\sigma} \leq 5$$

$$\phi_s = A_2 e^{-0.25(h/\sigma)} \qquad \text{for } \frac{h}{\sigma} > 5$$

where A_1, A_2, α_1, α_2, and α_3 are constants that can be found in [8].

Depending on the roughness configuration, ϕ_s can be positive, negative, or zero. To understand the physical significance of the sign of ϕ_s, let us assume surface j is moving and surface b is stationary (fig. 2). The additional flow transport due to the combined effect of roughness and sliding is $(u_j/2)\sigma\phi_s$. If surface j is rough, the fluid carried in the valleys results in an additional flow transport, thereby meaning a positive

ϕ_s. On the other hand, if surface j is smooth, the asperities of the stationary rough surface act as barriers in restricting the flow. This gives a decreased flow as revealed by a negative ϕ_s.

In the present case, when $V_{rj} = 1$, ϕ_s is positive, which means a rough moving surface and a smooth stationary surface. In other words the journal has a rough surface and the bearing a smooth one. When $V_{rj} = 0$, the journal will have a smooth surface and the bearing a rough one. When $V_{rj} = 0.5$, $\sigma_j = \sigma_b$. This means both the journal and bearing surfaces have equal roughness. In this particular case, there is no ϕ_s effect.

For the journal bearing shown in figure 1, when the journal is rotating with surface velocity u, it carries a hydrodynamic load w_h in addition to asperity contact load. Assuming h and ϕ_x are functions of x only (implying no misalignment) and using the following substitutions

$$\theta = \frac{x}{R}, \quad Y = \frac{y}{(L/2)}, \quad H = \frac{h}{C}, \quad \Lambda = \frac{C}{\sigma}, \quad P = \frac{pC^2}{6\eta uR}$$

we get

$$\phi_x H^3 \frac{\partial^2 P}{\partial \theta^2} + \left(\frac{D}{L}\right)^2 \phi_y H^3 \frac{\partial^2 P}{\partial Y^2} + 3\phi_x H^2 \frac{\partial P}{\partial \theta} \frac{\partial H}{\partial \theta} + H^3 \frac{\partial P}{\partial \theta} \frac{\partial \phi_x}{\partial \theta}$$

$$= \frac{1}{2}\left[1 + \operatorname{erf}\left(\frac{\Lambda H}{\sqrt{2}}\right)\right] \frac{\partial H}{\partial \theta} + \frac{1}{\Lambda} \frac{\partial \phi_s}{\partial \theta} (2V_{rj} - 1) \qquad (7)$$

Dimensionless mean film thickness H is given by

$$H = 1 + \epsilon \cos \theta$$

Thus $\partial H/\partial \theta = -\epsilon \sin \theta$, and equation (7) reduces to

$$\phi_x H^3 \frac{\partial^2 P}{\partial \theta^2} + \left(\frac{D}{L}\right)^2 \phi_y H^3 \frac{\partial^2 P}{\partial Y^2} - 3\phi_x H^2 \frac{\partial P}{\partial \theta} \epsilon \sin\theta + H^3 \frac{\partial P}{\partial \theta} \frac{\partial \phi_x}{\partial \theta}$$

$$= \frac{1}{2}\left[1 + \operatorname{erf}\left(\frac{\Lambda H}{\sqrt{2}}\right)\right](-\epsilon \sin\theta) + \frac{1}{\Lambda}\frac{\partial \phi_s}{\partial \theta}(2V_{rj} - 1) \qquad (8)$$

The boundary conditions are

$$\left.\begin{aligned} P &= 0 \quad \text{at} \quad \theta = 0 \\ P &= \frac{\partial P}{\partial \theta} = 0 \quad \text{at} \quad \theta = \theta_2 \\ \frac{\partial P}{\partial Y} &= 0 \quad \text{at} \quad Y = 0 \\ P &= 0 \quad \text{at} \quad Y = 1 \end{aligned}\right\} \qquad (9)$$

where θ_2 is the angular coordinate at which the film cavitates. These conditions are known as Reynolds boundary conditions.

For a particular set of values of L/D, ϵ, γ (i.e., ϕ_x, ϕ_y, and ϕ_s), V_{rj}, and Λ, equation (8) is solved numerically by finite difference methods with successive overrelaxation factor satisfying the above boundary conditions. The numerical calculation is done with an accuracy of 0.01 percent of the difference of integrated pressures of two successive iterations.

Calculation of Hydrodynamic Load

Knowing the hydrodynamic pressure distribution, we calculate the two components of hydrodynamic load

$$w_x = -2 \int_0^{L/2} \int_0^{\theta_2} pR \cos\theta \, d\theta \, dy$$

and (10)

$$w_y = 2 \int_0^{L/2} \int_0^{\theta_2} pR \sin\theta \, d\theta \, dy$$

or in dimensionless form

$$\left.\begin{aligned} W_x &= -\int_0^1 \int_0^{\theta_2} P \cos\theta \, d\theta \, dY \\ \text{and} \\ W_y &= \int_0^1 \int_0^{\theta_2} P \sin\theta \, d\theta \, dY \end{aligned}\right\} \qquad (11)$$

where

$$W_x = \frac{w_x C^2}{6\eta u L R^2}$$

and

$$W_y = \frac{w_y C^2}{6\eta u L R^2}$$

The integrations of equation (11) are performed numerically by Simpson's rule. The total hydrodynamic load W_h is

$$W_h = \sqrt{W_x^2 + W_y^2} \qquad (12)$$

where

$$W_h = \frac{w_h C^2}{6\eta u R^2 L}$$

The attitude angle ψ is

$$\psi = \tan^{-1}\left(\frac{W_y}{W_x}\right)$$

Calculation of Side Leakage

The bearing side leakage can be calculated from

$$q = -2 \int_0^{\theta_2} \phi_y \frac{h^3}{12\eta} \frac{\partial p}{\partial y} R \, d\theta \tag{13}$$

or

$$Q = - \int_0^{\theta_2} \phi_y H^3 \frac{\partial P}{\partial Y} \, d\theta \tag{14}$$

where

$$Q = \frac{\left(\frac{L}{D}\right) q}{CRu} \tag{15}$$

The differentiation $\partial P/\partial Y$ of equation (14) is obtained numerically by the 3-point backward difference rule, and then the integration is performed numerically by Simpson's rule.

Calculation of Asperity Contact Load

By using a Gaussian distribution of asperity height, the contact load can be evaluated from nominal contact pressure. When both surfaces are rough, the nominal contact pressure given by Greenwood and Tripp [4] is

$$p_c = KE' F_{5/2} \tag{16}$$

where

$$K = \frac{8\sqrt{2}}{15} \pi (n\beta\sigma)^2 \sqrt{\frac{\sigma}{\beta}}$$

and

$$F_{5/2} = \frac{1}{\sqrt{2\pi}} \int_{\Lambda}^{\infty} (s - \Lambda)^{5/2} e^{-s^2/2} \, ds$$

The function $F_{5/2}$ has been calculated in [4] for various Λ and tabulated, and K can be calculated for a particular σ/β from the above expression.

The contact load is

$$W_c = LDp_c$$

or

$$W_c = KF_{5/2} \tag{17}$$

where

$$W_c = \frac{W_c}{LDE'} \tag{18}$$

The two dimensionless loads W_h and W_c are defined in such a way that they cannot be simply added. In the following section a numerical example is taken to show the procedure for calculating these loads.

Example

An oil journal bearing is operating under the following conditions:

Diameter of journal $D = 50$ mm

Length of bearing $L = 50$ mm

Radial clearance $C = 0.025$ mm

Eccentricity ratio $\epsilon = 0.8$

Journal speed $u = 5$ m/s

Absolute viscosity oil $\eta = 0.01$ N s/m^2

Assume $E' = 2.2 \times 10^{11}$ N/m^2 and $\sigma/\beta = 0.01$. Find the contact load and the hydrodynamic load.

Although $F_{5/2}$ will be different for different h, $F_{5/2}$ at $h = h_{min}$ is used.

$$h_{min} = C(1 - \epsilon)$$

Substituting the values of C and ϵ,

$$h_{min} = 0.0050 \text{ mm}$$

The contact load is

$$w_c = LDKE'F_{5/2}$$

Substituting the values of D and L and taking $K = 0.003$ give

$$W_c = 165 \times 10^4 \text{ N}$$

Assume a roughness parameter Λ of 1. The function $F_{5/2}$ corresponding to $\Lambda = 1$ is 0.08056 [4]. Thus the contact load w_c is 133 kN.

It is further assumed that both journal and bearing surfaces have the same roughness structure and that the surface roughness pattern is isotropic. From figure 3 the dimensionless hydrodynamic load for the above bearing is $W_h = 2.6$.

Hence the hydrodynamic load is given by

$$w_h = \frac{6\eta LR^2 u\, W_h}{C^2}$$

Substituting the above data in this expression yields

$$w_h = 39 \text{ kN}$$

The ratio of contact to hydrodynamic load is

$$\frac{w_c}{w_h} = 3.41$$

RESULTS AND DISCUSSION

The hydrodynamic load, attitude angle, and side leakage in dimensionless form are computed for various length-to-diameter ratios (0.5, 1.0, and 2.0), eccentricity ratios (0.2, 0.4, 0.6, and 0.8), roughness parameters (1, 2, 3, 4, and 6), surface pattern parameters (1/6, 1, and 6), and variance ratios (0, 0.5, and 1.0). These data cover a wide range of design variables used in practice. The results are shown in tables I and II and figures 3 to 9. In the discussion to follow, the hydrodynamic load and side leakage will be termed simply as load and flow, respectively. Using Patir and Cheng [8] shear stress factors, the frictional force on the journal surface was computed. The frictional forces at some eccentricity ratios were unrealistic. Hence they are not reported herein.

In table I the performance characteristics of a finite journal bearing calculated from the present method of solution for smooth surface bearings ($\Lambda = 6$) are compared with a similar available solution [9]. For $\epsilon = 0.8$ the agreement is not as good as for lower eccentricity ratios.

A parametric study of the bearing characteristics is made in the following paragraphs.

Effect of roughness parameter Λ. - The variation of load, attitude angle, and flow of a bearing having $L/D = 1.0$ and $\gamma = 1$ is shown as a function of roughness parameter in figures 3 to 5 for various eccentricity ratios and variance ratios. The load and flow increase but attitude angle decreases with increasing eccentricity ratio. This is a typical characteristic of a hydrodynamic oil journal bearing under steady-state conditions.

When both journal and bearing have the same roughness structure (i.e., $V_{rj} = 0.5$), load increases; flow decreases with increasing roughness

(i.e., for small Λ). The attitude angle remains more or less constant with roughness parameter for the same configuration.

When the journal surface is rough and the bearing surface is smooth (i.e., $V_{rj} = 1.0$), ϕ_s is positive. This makes the last term on the right side of the Reynolds equation positive, thereby giving less pressure. Hence load decreases with increasing roughness. But for smaller values of Λ ($\Lambda < 2$), the load increases. This strange behavior of W_h for small Λ can be understood by looking carefully at the expression for ϕ_s. If ϕ_s is plotted against Λ, it will be seen that ϕ_s increases with Λ to start with and then decreases as Λ is further increased and will approach 0 when Λ is very large. At smaller values of Λ the number of contact points increases, and these points permit little or no flow in the direction of motion thereby increasing pressure and hence load.

On the other hand, when the journal surface is smooth and the bearing is rough (i.e., $V_{rj} = 0$), ϕ_s is negative. We expect load behavior just opposite to that of $V_{rj} = 1.0$. This, in fact, is shown in figure 3 for $V_{rj} = 0$. Thus we get some intermediate values of load when $V_{rj} = 0.5$ if other parameters are kept constant.

From figure 4 it can be seen that for small ε (0.2), the attitude angle is not influenced much by Λ. For a higher value of ε (0.8), the attitude angle for $V_{rj} = 1.0$ drops sharply at small Λ and becomes negative when $\Lambda = 1$.

The side leakage is plotted against roughness parameter for various ε and V_{rj} in figure 5. When $V_{rj} = 0.5$, the side leakage decreases with increasing roughness. As the roughness is increased, these is a likelihood of more asperity contacts. This restricts the flow. Under this situation ($V_{rj} = 0.5$), it may be noted that the load increases (fig. 3). When

$\gamma = 1$, $\phi_x = \phi_y$. Therefore when V_{rj} is 1.0 or 0, we expect a somewhat similar behavior of flow with load (flow is dependent on ϕ_y). The present results (fig. 5) show the similar trend.

Effect of surface pattern parameter γ. - The load and flow are shown (figs. 6 and 7) with respect to roughness parameter for various surface pattern parameters and eccentricity ratios. The ϕ_x is higher for longitudinally oriented surfaces ($\gamma > 1$) and lower for transversely oriented surfaces ($\gamma < 1$) than for isotropic surfaces ($\gamma = 1$). Again $\phi_y(\Lambda H, \gamma) = \phi_x(\Lambda H, 1/\gamma)$. As load is a function of both ϕ_x and ϕ_y and as both ϕ_x and ϕ_y are related to γ in such a way, it is quite difficult to foresee the optimum values of load and flow for a particular γ. From figures 6 and 7 it is observed that for a small eccentricity ratio ($\varepsilon = 0.2$), the maximum load and minimum side leakage Q are given by $\gamma = 6$ for $L/D = 1.0$ and $V_{rj} = 0.5$. For the same bearing configuration, when $\varepsilon = 0.6$, the isotropic surface gives maximum load, but the flow is minimum for a surface having $\gamma = 6$.

Effect of length-to-diameter ratio L/D. - In figures 8 and 9 the performance behavior for various L/D and ε with $V_{rj} = 0.5$ and $\gamma = 1$ is shown. As expected, a bearing with higher L/D and ε gives higher load and lower flow q. In table II the load and side leakage for various L/D ratios and γ with $\varepsilon = 0.2$ is given. As mentioned earlier, ϕ_x, ϕ_y, and γ are related in such a way that it is extremely difficult to predict which particular bearing configuration, so far as L/D and γ are concerned, gives maximum load and minimum side leakage. In view of this, a large amount of data was generated and tabulated (table II). It can be seen from table II that, when both journal and bearing surfaces have identical roughness structures, a bearing with $L/D = 2.0$ and $\gamma = 1$ gives maximum

load, but a bearing with $L/D = 0.5$ and $\gamma = 6$ gives minimum side leakage. However, the flow in this case will not be minimum, since Q is non-dimensionalized with L/D. The minimum absolute side leakage q will, of course, be given by a bearing having $L/D = 0.5$ and $\gamma = 6$ under such an operating condition.

CONCLUSIONS

By using a flow simulation model developed by Patir and Cheng [5], the steady-state performance behavior of a finite oil journal bearing using Reynolds boundary conditions was obtained. From this study and the results presented the following conclusions were drawn:

1. When the roughness parameter Λ is 6, the results (smooth surface solution) obtained from the present method of solution are in reasonably good agreement with the similar available solution.

2. The hydrodynamic load increases and dimensionless side leakage decreases with increasing surface roughness when both journal and bearing surfaces have the same roughness structure.

3. When the journal surface is very rough ($\Lambda < 2$) and the bearing surface is smooth, the load capacity and side leakage Q are higher for surfaces having the same roughness structure.

4. When the bearing surface is very rough ($\Lambda < 2$) and the journal surface is smooth, the load capacity and side leakage Q are lower for surfaces having the same roughness structure.

5. The values of hydrodynamic load and side leakage Q for bearings having the same roughness structure on both surfaces are in between the values for the bearings having rough journal surfaces and the values for bearings having rough bearing surfaces.

6. When both surfaces have the same roughness structure and when the bearing operates under lightly loaded conditions, a bearing with a longitudinally oriented surface pattern gives maximum load and side leakage, and a bearing with a transversely oriented surface pattern gives minimum load and side leakage.

7. The contact load of a partially lubricated surface can sometimes be comparable to hydrodynamic load.

REFERENCES

1. Greenwood, J. A.; and Williamson, J. B. P.: Contact of Nominally Flat Rough Surfaces. Proc. R. Soc. (London), vol. A295, no. 1442, Dec. 1966, pp. 300-319.

2. Whitehouse, D. J.; and Archard, J. F.: The Properties of Random Surfaces of Significance in Their Contact. Proc. R. Soc. (London), vol. A316, no. 1524, Mar. 1970, pp. 97-121.

3. Nayak, P. R.: Random Process Model of Rough Surfaces. J. Lubr. Technol., vol. 93, no. 3, July 1971, pp. 398-407.

4. Greenwood, J. A.; and Tripp, J. H.: The Contact of Two Nominally Flat Rough Surfaces. Proc. Inst. Mech. Eng. (London), vol. 185, 1970-71, pp. 625-633.

5. Patir, N.; and Cheng, H. S.: An Average Flow Model for Determining Effects of Three-Dimensional Roughness on Partial Hydrodynamic Lubrication. J. Lubr. Technol., vol. 100, no. 1, Jan. 1978, pp. 12-17.

6. Tønder, K.: Simulation of the Lubrication of Isotropically Rough Surfaces. ASLE Trans., vol. 23, no. 3, July 1980, pp. 326-333.

7. Majumdar, B. C.; and Hamrock, B. J.: Effect of Surface Roughness on Hydrodynamic Bearings. NASA TM-81711, 1981.

8. Patir, N.; and Cheng, H. S.: Application of Average Flow Model to Lubrication Between Rough Sliding Surfaces. J. Lubr. Technol., vol. 101, no. 2, Apr. 1979, pp. 220-230.

9. Pinkus, O.; and Sternlicht, B.: Theory of Hydrodynamic Lubrication. McGraw Hill Book Co., Inc., 1961, p. 86.

TABLE I. - COMPARISON OF HYDRODYNAMIC LOAD CAPACITY, ATTITUDE ANGLE, AND SIDE LEAKAGE WITH AVAILABLE SMOOTH SURFACE BEARING SOLUTION

[L/D = 1.0, Λ = 6, V_{rj} = 0.5.]

ϵ	W_{ll} (load)	ψ° (attitude angle)	Q (side leakage)
0.2	0.08 (0.08)*	73.6 (74)	0.31 (0.32)
.4	.19 (.20)	61.6 (62)	.61 (.61)
.6	.45 (.44)	48.6 (50)	.93 (.94)
.8	1.46 (1.18)	33.3 (36)	1.29 (1.24)

*Values in parentheses are from Pinkus and Sternlicht [9] (table 4-1) p. 86.

TABLE II. - VARIATION OF HYDRODYNAMIC LOAD AND SIDE LEAKAGE WITH VARIOUS LENGTH-TO-DIAMETER RATIOS AND SURFACE PATTERN PARAMETERS

[$\epsilon = 0.2$, $V_{rj} = 0.5$.]

L/D	γ	Λ	W_h	Q
0.5	1/6	1	0.013	0.08
		2	.020	.09
		3	.022	.09
		4	.022	.09
	1	1	0.044	0.07
		2	.032	.09
		3	.028	.09
		4	.026	.09
	6	1	0.104	0.04
		2	.050	.08
		3	.036	.08
		4	.030	.09
1.0	1/6	1	0.054	0.32
		2	.074	.35
		3	.075	.33
		4	.075	.32
	1	1	0.131	0.28
		2	.105	.30
		3	.091	.31
		4	.084	.31
	6	1	0.157	0.09
		2	.127	.22
		3	.105	.27
		4	.097	.28
2.0	1/6	1	0.203	1.28
		2	.209	1.08
		3	.209	1.01
		4	.196	.94
	1	1	0.309	0.69
		2	.247	.80
		3	.215	.82
		4	.197	.82
	6	1	0.210	0.12
		2	.211	.49
		3	.202	.64
		4	.192	.71

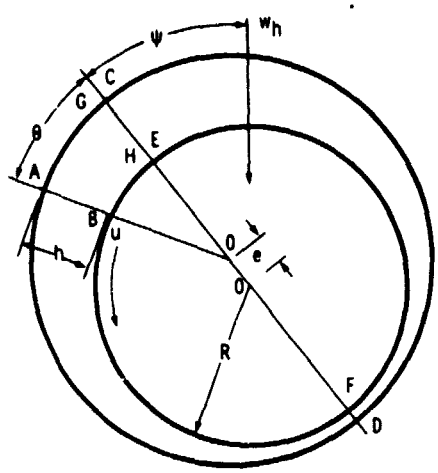

Figure 1. - Diagram of an oil journal bearing with a greatly exaggerated clearance.

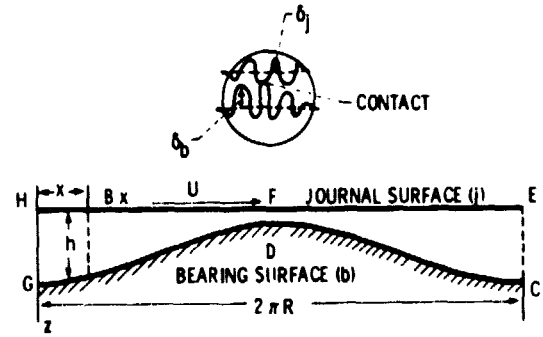

Figure 2. - Developed journal and bearing surfaces of a finite oil journal bearing.

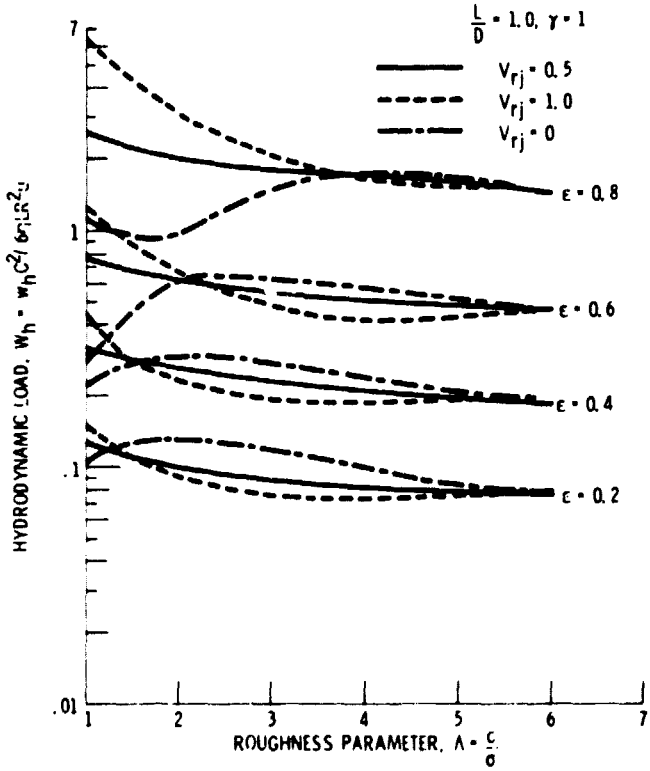

Figure 3. - Variation of hydrodynamic load with roughness parameter for various eccentricity ratios and variance ratios.

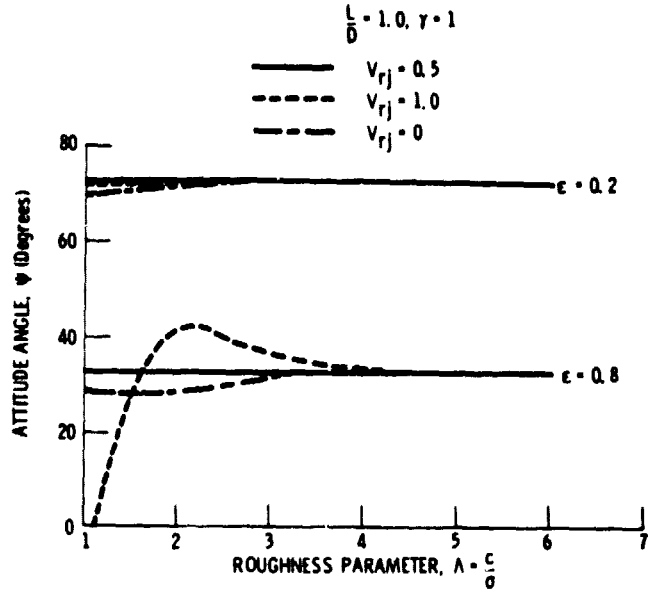

Figure 4. - Variation of attitude angle with roughness parameter for various eccentricity ratios and variance ratios.

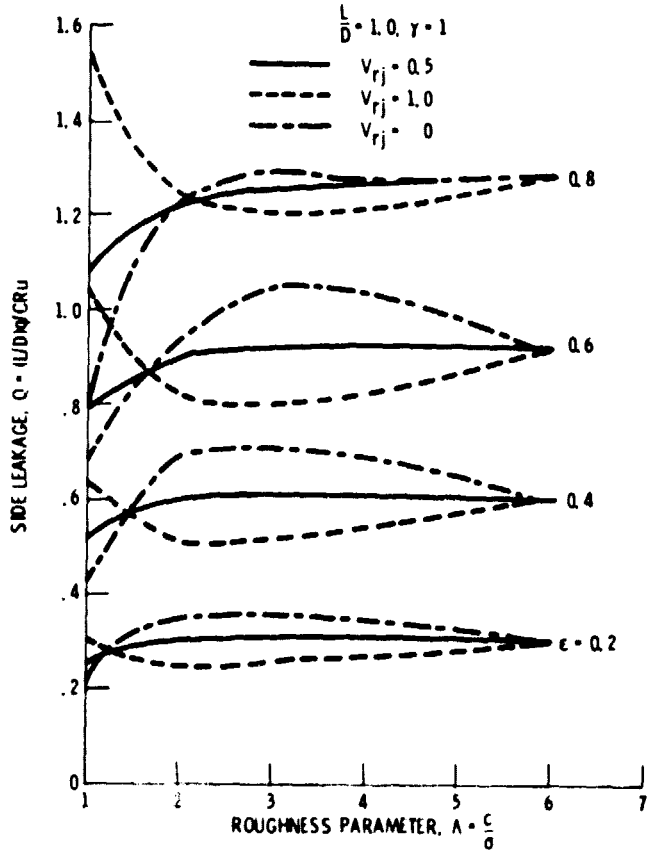

Figure 5. - Variation of side leakage with roughness parameter for various eccentricity ratios and variance ratios.

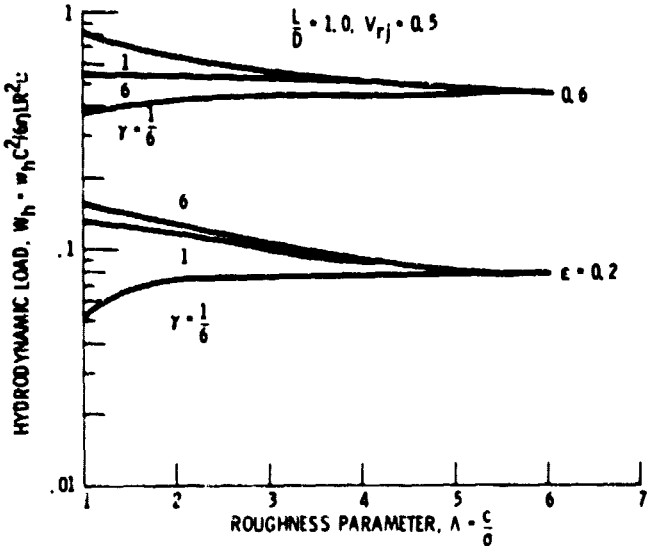

Figure 6. - Variation of hydrodynamic load with roughness parameter for various roughness pattern parameters.

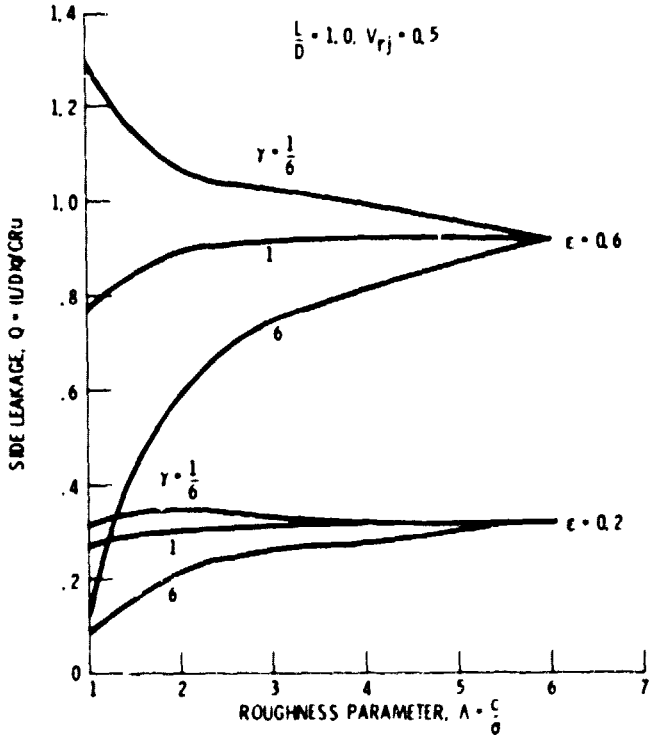

Figure 7. - Variation of side leakage with roughness parameter for various roughness pattern parameters.

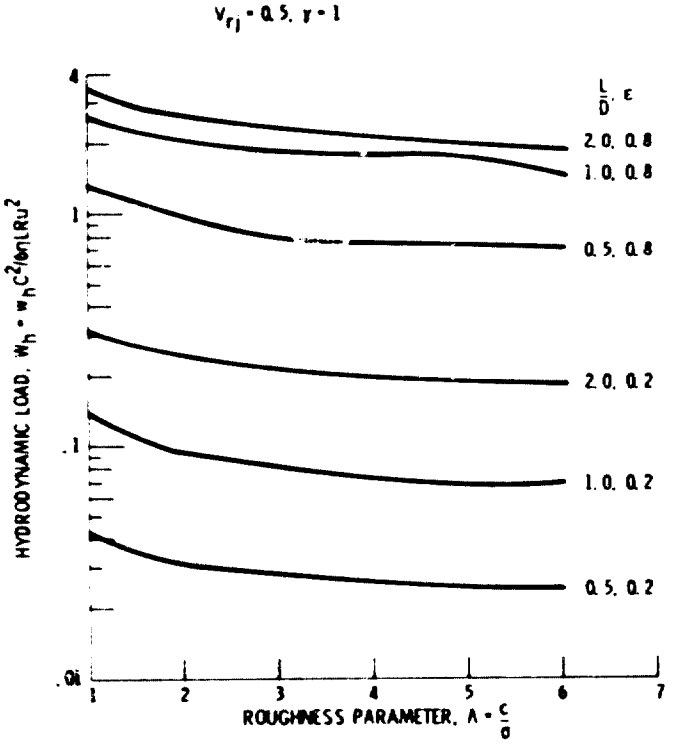

Figure 8. - Variation of hydrodynamic load with roughness parameter for various length-to-diameter ratios.

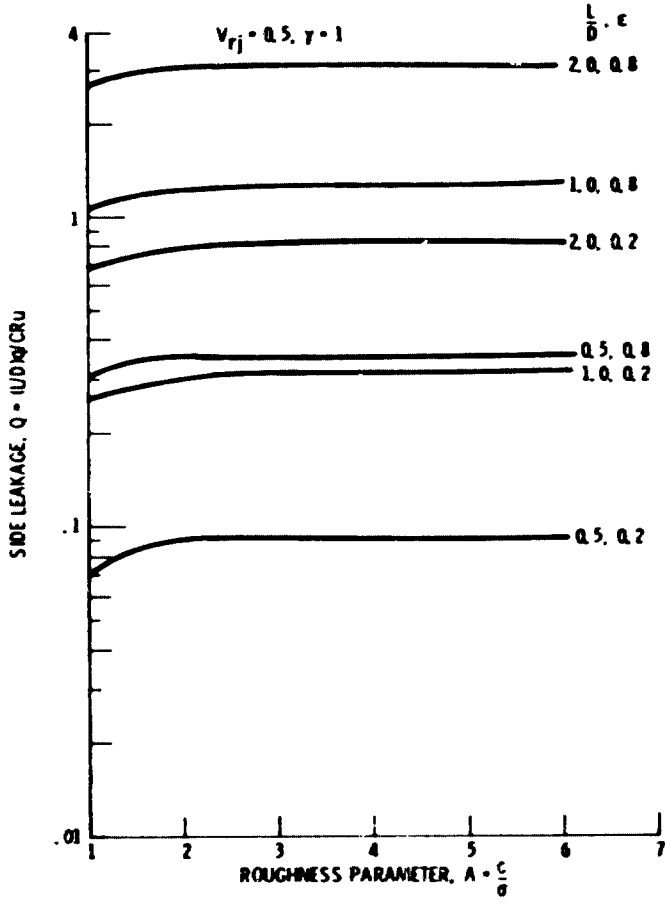

Figure 9. - Variation of side leakage with roughness parameter for various length-to-diameter ratios.